

Rational Design, Synthesis and Evaluation of Oxazolo[4,5-c]-quinolinone Analogs as Novel Interleukin-33 Inhibitors

Yujin Kim^{+, [a]}, Chao Ma^{+, [a, e]}, Seonghu Park,^[a] Yujin Shin -,^[a] Taeyun Lee,^[a] Jiwon Paek,^[a] Kyong Hoon Kim,^[b] Geonhee Jang,^[a] Haelim Cho,^[c] Seyoung Son,^[d] Sang-Hyun Son,^[d] Ki Yong Lee,^[a] Kiho Lee,^[a] Yong Woo Jung,^{*, [a]} Young Ho Jeon,^{*, [a]} and Youngjoo Byun^{*, [a]}

Abstract: Interleukin-33 (IL-33) is an epithelial-derived cytokine that plays an important role in immune-mediated diseases such as asthma, atopic dermatitis, and rheumatoid arthritis. Although IL-33 is considered a potential target for the treatment of allergy-related diseases, no small molecule that inhibits IL-33 has been reported. Based on the structure-activity relationship and in vitro 2D NMR studies employing ¹⁵N-labeled IL-33, we identified that the oxazolo[4,5-c]-

quinolinone analog **7c** binds to the interface region of IL-33 and IL-33 receptor (ST2), an orphan receptor of the IL-1 receptor family. Compound **7c** effectively inhibited the production of IL-6 in human mast cells in a dose-dependent manner. Compound **7c** is the first low molecular weight IL-33 inhibitor and may be used as a prototype molecule for structural optimization and investigation of the IL-33/ST2 signaling pathway.

Introduction

Interleukin-33 (IL-33), a member of the IL-1 family of cytokines, is constitutively expressed and secreted from epithelial and endothelial cells into extracellular spaces during tissue damage and necrosis.^[1] After release, IL-33 binds strongly to a heterodimeric receptor complex consisting of the IL-33-specific primary receptor ST2 (also known as IL-1RL1) and a ubiquitously expressed IL-1R accessory protein (IL1RAcP).^[2] ST2 is preferentially expressed on the surface of Th2 cells, mast cells, basophils, eosinophils, natural killer cells, and type 2 innate lymphoid cells (ILC2).^[3] Upon binding to the appropriate ligand, ST2 subsequently recruits MyD88, which leads to a downstream signaling cascade that activates the NF- κ B and MAPK pathways.^[4] A number of reports have highlighted the fact that the IL-33/ST2 signal transduction pathway is closely associated with host defense and immune regulation in inflammatory and infectious diseases.^[5] Moreover, it has been suggested that IL-33 works as an alarmin by releasing danger signal substances under stress conditions; therefore, this cytokine may play a pivotal role in mediating pathological signaling of the onset of aforementioned diseases.^[3b,4,6] Hence, IL-33 is considered an important and novel target for therapeutic intervention in a wide range of immune-mediated diseases including allergies, asthma, cardiovascular dis-

ease, and other autoimmune disorders. However, their precise functions of IL-33 and underlying mechanisms in the development of these diseases are still not fully understood. Therefore, there is clearly a need for more research in the fields of molecular biology, genetics, immunology, and other related disciplines to elucidate the enigmatic biological implications of the IL-33/ST2 signaling pathway in these diseases. Furthermore, small molecule inhibitors targeting IL-33 would be highly useful for the investigation of IL-33/ST2 signaling in processes related to the inflammatory and autoimmune diseases.

Despite the great interest in IL-33 as a therapeutic target, there have been no reports on small molecules that effectively inhibit IL-33. We previously reported that BTB11086 (2-phenyl-5H-[1,3]oxazolo [4,5-c]quinolin-4-one) binds to the hydrophobic pocket of IL-33 and might block the IL-33/ST2 interactions.^[7] Although it was a very weak inhibitor of IL-33, it represents a promising starting point for developing novel and potent IL-33 inhibitors. Herein we designed, synthesized, and evaluated a series of novel oxazolo[4,5-c]-quinolinone analogs as the first examples of small-molecule inhibitors of IL-33.

[a] Y. Kim,⁺ C. Ma,⁺ S. Park, Y. Shin -, T. Lee, J. Paek, G. Jang, Prof. K. Yong Lee, Prof. K. Lee, Prof. Y. Woo Jung, Prof. Y. Ho Jeon, Prof. Y. Byun
College of Pharmacy Korea University
2511 Sejong-ro, Sejong 30019 (South Korea)
E-mail: yjung@korea.ac.kr
yhjeon@korea.ac.kr
yjbyun1@korea.ac.kr


[b] K. Hoon Kim
Department of Biotechnology and Bioinformatics
Korea University
Sejong 30019 (South Korea)

[c] H. Cho
T&J TECH Inc.
212 Gasan digital 1-ro, Geumcheon-gu, Seoul 08502 (South Korea)

[d] S. Son, S.-H. Son
Azcuris, Co., Ltd.
2511 Sejong-ro, Sejong 30019 (South Korea)

[e] C. Ma⁺
Current address
College of Food & Pharmaceutical Engineering
Guizhou Institute of Technology
Guizhou 550003 (P. R. China)

[*] These authors contributed equally.

 This manuscript is part of a special collection celebrating the 75th Anniversary of the Korean Chemical Society.

Results and Discussion

Structural analysis of IL-33 and BTB11086 interaction

We analyzed the binding interfaces of the IL-33/ST2 system in order to gain insights on making BTB11086 derivatives. Among the binding interfaces between IL-33 and the ST2 receptor in the complex structure (PDB ID: 4KC3),^[8] we focused on the hydrophobic pocket of IL-33, which interacts with the 3rd immunoglobulin-like domain of the ST2 receptor (residues Gly 207 to Arg 317 in ST2) (Figure 1A). The IL-33 hydrophobic pocket consists of β -strands (β 1, β 5, β 6, β 9, β 10 and β 13) that form a barrel-like structure. The inner surface of the barrel-like pocket has a number of hydrophobic residues (Tyr 122, Ala 124, Leu 161, Tyr 163, Leu 182, Val 184, Leu 220, Val 228, and Leu 267) and a few polar residues (Asn 222, Asn 226 and Ser 268). Docking studies of BTB11086 with IL33 suggested that this compound interacts with the surface of IL33 via a combination of hydrophobic interactions with Ala 124, Leu 220 and Phe 230, and polar interactions with Asn 222 and Asn 226. Based on the best-docked pose of BTB11086 (Figure 1B), we designed a series of new IL-33 inhibitors by introducing 2-(dialkylamino)ethyl groups at the 4- or 5-position of the oxazolo[4,5-*c*]-quinolinone scaffold, which was expected to make additional interactions with the hydrophilic amino acids (His 224 and Asn 226) of IL-33.

Synthetic Chemistry

Oxazolo[4,5-*c*]-quinolinone analogs were prepared from commercially available ethyl 2-aminoxazole-4-carboxylate in six synthetic steps as shown in Scheme 1. Synthesis of the key intermediates **5a–5e** was achieved according to a published method with some modifications.^[9] Briefly, ethyl 2-aminoxazole-4-carboxylate was transformed into compound **1** by applying the Sandmeyer reaction.^[10] Substitution at the 2-position of the oxazole ring with a 4-substituted phenyl group by using the Suzuki-Miyaura cross-coupling reaction afforded compounds **2a–2e** in 54–90% yield. Subsequently, the *o*-nitrophenyl group was introduced at the 5-position of the

oxazole **2** through the palladium-catalyzed Heck reaction. Reaction of **2a–2e** with 2-iodonitrobenzene under standard palladium-catalyzed conditions [Pd(OAc)₂/PPh₃/Cs₂CO₃/DMF] provided compounds **3a–3e** in 32–67% yield. The nitro group of **3a–3e** was reduced to the corresponding amines **4a–4e** under hydrogenation conditions (10% Pd/C, H₂). Without purification of compounds **4a–4e**, ring cyclization under basic conditions afforded the oxazolo[4,5-*c*]-quinolinone compounds **5a–5e** in 60–82% yield. With the key intermediates **5a–5e** in hand, alkylation reactions of **5a–5e** were carried out with 2-(dimethylamino)ethyl bromide under basic conditions (K₂CO₃, DMF) at 130 °C. Alkylation of the quinolinone compounds provided a mixture of both *N*- and *O*-alkylated products due to the keto-enol tautomeric equilibrium.^[11] However, TLC analysis of the reaction mixture revealed three major spots. The respective spots were isolated by column chromatography on silica gel using gradient elution with a methanol/ether system (1:10 to 1:3). The chemical structures of the three spots were analyzed by ¹H and ¹³C NMR spectroscopy along with extensive 2D NMR experiments. The ¹³C NMR spectra of the compounds in CDCl₃ showed carbon peaks corresponding to CH₂ at 37.6 ppm for the *N*-alkylated products **6a–6e** (bottom spot on TLC) and those at 64.2 ppm for the *O*-alkylated products **7a–7e** (middle spot). Furthermore, these assignments were confirmed by NOESY experiments, based on the connection of the cross-peaks of the methylene protons of the *N,N*-dimethylaminoethyl moiety (δ =3.87) and the proton at the C-8 position of the quinolinone ring (See supplementary data). ¹H NMR analysis of the fast-eluting top spot on TLC showed the presence of a singlet peak at δ =3.91 ppm which exhibited NOESY cross-coupling with the C-8 position of the quinolinone ring (See supplementary data), implying that the methyl group is attached to an amide nitrogen of the quinolinone ring as shown in compounds **8a–8e** (Scheme 1). To investigate whether a similar alkylation occurs with different alkylating agents, 2-(diethylamino)ethyl bromide hydrobromide was subjected to alkylation with **5a** under the same reaction conditions as shown in Scheme 2. However, only compounds **9a** and **9b** were obtained in low yield without any trace of the *N*-ethylated product. It is assumed that the *N*-methylated products **8a–8e** might be generated by the formation of quaternary ammonium salts from self-reaction of the less bulky 2-(dimethylamino)ethyl bromide and subsequent S_N2 reaction with the quinolinone ring at high temperature.

NMR binding study of oxazolo[4,5-*c*]-quinolinone analogs with IL-33

To screen the interaction of the synthesized compounds with IL-33, a series of NMR binding studies were performed based on chemical shift perturbations (CSPs) in the ¹H-¹⁵N HSQC spectra of the ¹⁵N-labeled IL-33 protein. The previously reported backbone NMR signals of IL-33 were obtained from the Biological Magnetic Resonance Bank (www.bmrb.wisc.edu).^[12] The CSPs of the NMR signals of the backbone amide of the key residues in the hydrophobic pocket of IL-33 were monitored with the

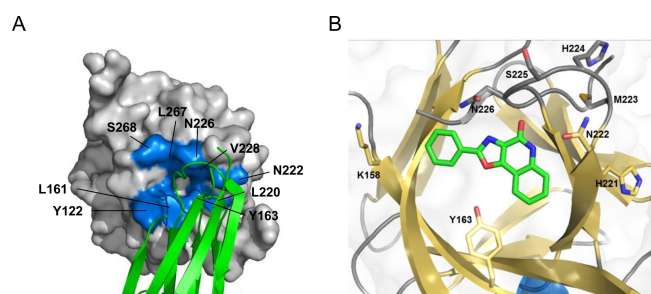
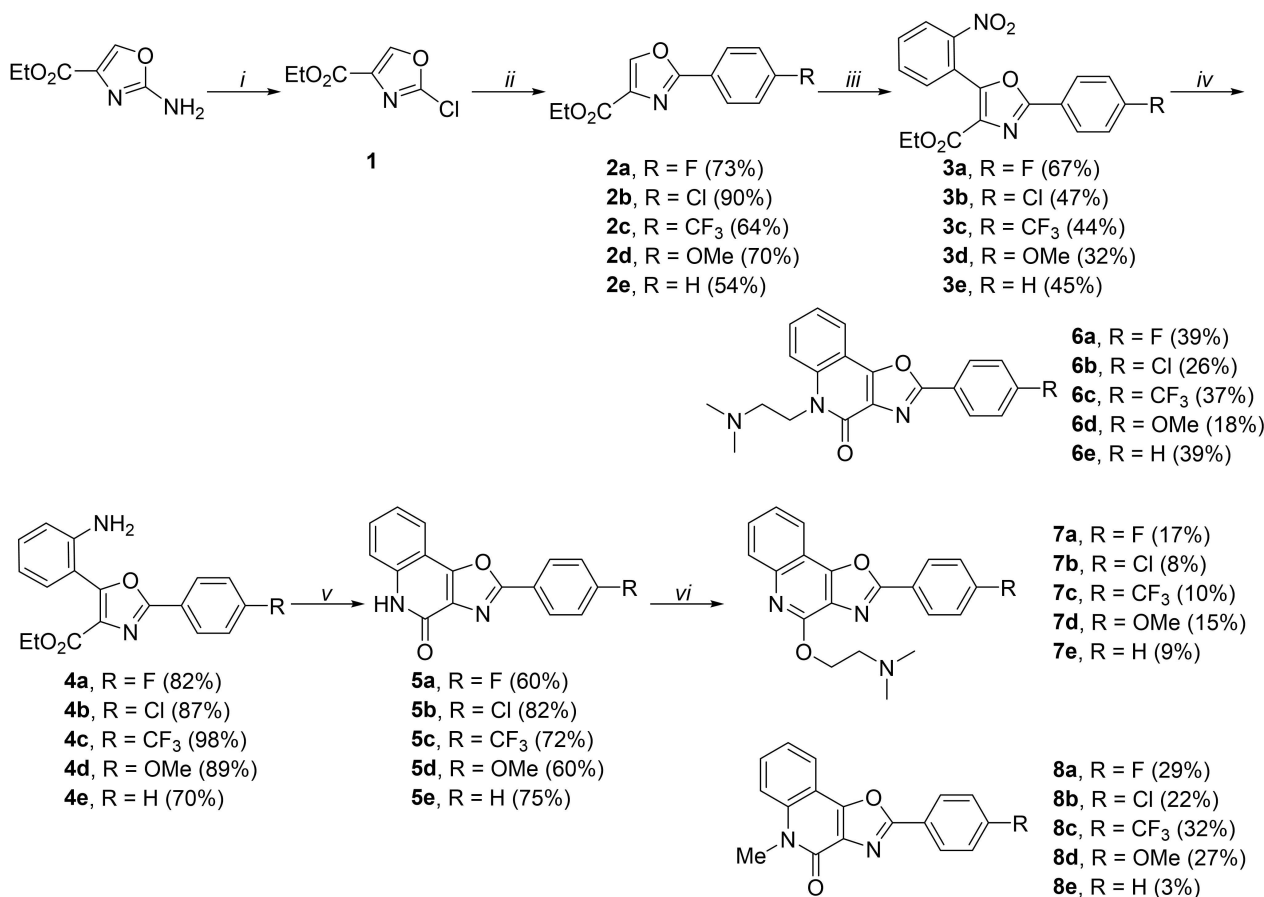
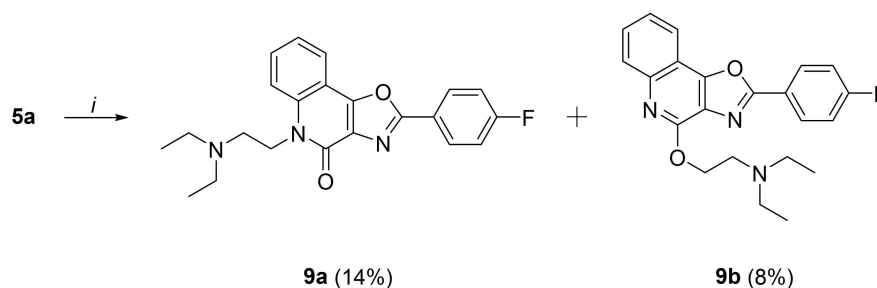


Figure 1. Structural analysis of interaction between IL-33 and BTB11086. (A) Structure of IL-33 in complex with ST2 (PDB ID: 4KC3). The hydrophobic surface of IL-33, which is the interface for ST2 binding, was exploited to discover the inhibitor. Amino acid residues in the binding interface are denoted as blue. (B) Docked pose of BTB11086 on the hydrophobic pocket of IL-33. BTB11086 formed hydrogen bonds with Asn 222 and Asn 226, and hydrophobic contacts with Ala 124, Leu 220, and Leu 267.



^a Reagents and Conditions : (i) *t*-BuONO, CuCl₂, acetonitrile, 80 °C, 2 h, (64%); (ii) *p*-RPhB(OH)₂, Pd(PPh₃)₄, PhMe, H₂O, K₂CO₃, 90 °C, 1 h; (iii) 2-IC₆H₄NO₂, Pd(OAc)₂, PPh₃, Cs₂CO₃, DMF, 140 °C, 3 h; (iv) 10% Pd/C, MeOH, H₂, 1 h; (v) DMF, H₂O, 2 M K₂CO₃, 90 °C, 12 h; (vi) (CH₃)₂NCH₂CH₂Br·HBr, K₂CO₃, DMF, 130 °C, 3 h.

Scheme 1. Synthesis of oxazolo[4,5-*c*]quinolinone analogs with 2-(dimethylamino)ethyl substituent (**6a–7e**).



Reagents and Conditions : (i) (CH₂CH₃)₂NCH₂CH₂Br·HBr, K₂CO₃, DMF, 130 °C, 5 h

Scheme 2. Synthesis of oxazolo[4,5-*c*]quinolinone analogs with 2-(diethylamino)ethyl substituent (**9a–9b**).

addition of the synthesized analogs as well as BTB11086 (**5e** in Scheme 1). Mapping of the residues was achieved by monitoring amide signals perturbed by the binding of the compounds. Figure 2A shows an example of the perturbations in the ¹H-¹⁵N HSQC experiment for ¹⁵N-labeled IL-33 by the addition of the compound **7c**. The superimposed spectra of IL-33 in the absence (black) and the presence (red) of **7c**, showed that

several NMR signals of IL-33 were selectively broadened or shifted. This might be due to a change of the chemical environment upon binding of compound **7c** or due to the exchange of IL-33 between the free and bound states on the NMR chemical shift time-scale. The perturbed signals correspond to the residues involved in the direct binding or the conformational change induced by the binding of **7c**. All of the

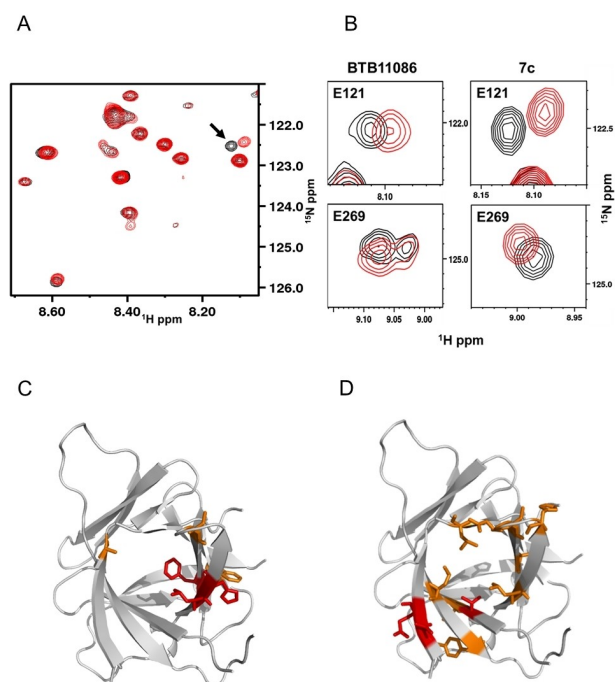


Figure 2. NMR binding studies of interaction of the oxazolo[4,5-*c*]-quinolinone analogs with IL-33: (A) ^1H - ^{15}N HSQC superimposed spectra of IL-33 in the absence (black) and the presence (red) of compound **7c**. (B) ^1H - ^{15}N HSQC superimposed sub-spectra of IL-33 showing the chemical shift perturbations of the Glu 121 (upper spectra) and Glu 269 (lower spectra) backbone amide signals due to the binding of BTB11086 (left) and **7c** (right). Black and red contours represent the IL-33 signals in the absence and presence of the compounds, respectively. (C) Mapping of the perturbed residues on the backbone structure of IL-33 due to the binding of BTB11086. (D) Mapping of the perturbed residues on the backbone structure of IL-33 due to the binding of **7c**. Relatively strong and weak perturbation residues are marked in red and orange, respectively.

synthesized compounds were screened using ^1H - ^{15}N HSQC experiments and most of them showed moderate perturbations due to binding to the hydrophobic pocket on IL-33. To ensure that the binding sites were identical for the same binding mode of the synthesized compounds, we used the CSP values of Glu 121 for which there was a significant shift. All of the *N*- and *O*-alkylated compounds (**6a–7e**) showed CSPs greater than that of **5e**, as summarized in Table 1. The representative spectra of **7c**, showing a comparison of the CSPs of Glu 121 and Glu 269 versus that of BTB11086, are presented in Figure 2B. Compound **7c** induced stronger perturbation of the CSPs at both Glu 121 and Glu 269 sites than **5e**. The amino acid residues in the IL-33 and ST2 binding interface which showed CSPs of the NMR signals upon interaction with **7c** were Thr 120, Glu 121, Leu 161, Leu 220, His 224, Asn 226, Cys 227, Ser 229, Leu 267, and Glu 269 (See supplementary data). Although Val 184 and Thr 185 were not exposed on the binding interface, they were also perturbed possibly by the secondary effect of the binding of **7c**. The residues perturbed by the addition of **5e** and **7c** are indicated by red and orange coloration on the backbone structure of IL-33, respectively (Figure 2C-2D).

Comparative molecular field analysis (CoMFA) of oxazolo [4,5-*c*]-quinolinone analogs

Based on the extent of the CSPs for the selected residue Glu 121, comparative molecular field analysis (CoMFA) of the synthesized IL-33 inhibitors was performed using the SYBYL-X 2.1.1 module (Tripos Inc., St. Louis, MO, USA). All analogs except for **4c** commonly possess the oxazolo[4,5-*c*]quinolinone scaffold. The results of partial least square (PLS) analysis of the CoMFA model are summarized in Table 2. The cross-validated coefficient (q^2) and non-cross-validated coefficient (r^2) values were 0.767 and 0.961, respectively, with the optimum number of components of 3; SEP,

Table 1. Actual and CoMFA-predicted $\log(\text{CSP}) + 4$ value of compounds in the training set and test sets.

Entry	ID	CSP	Actual $\log(\text{CSP}) + 4$	Predicted $\log(\text{CSP}) + 4$	Residual
Training set					
1	3c	0.0009	0.9621	0.8935	0.0686
2	5a	0.0027	1.4241	1.4668	-0.0427
3	5b	0.0034	1.5324	1.4237	0.1087
4	5c	0.0023	1.3584	1.3829	-0.0245
5	5e	0.0032	1.5094	1.4812	0.0282
6	6a	0.0804	2.9053	2.5949	0.3104
7	6b	0.0367	2.5652	2.5517	0.0134
8	6c	0.0366	2.5633	2.5548	0.0085
9	6d	0.0177	2.2479	2.3568	-0.1089
10	6e	0.0348	2.5414	2.6094	-0.0680
11	7c	0.0218	2.3386	2.3956	-0.0570
12	7d	0.0103	2.0122	2.2269	-0.2147
13	7e	0.0326	2.5129	2.4564	0.0565
14	8c	0.0023	1.3584	1.4370	-0.0786
Test set					
15	4c	0.0009	0.9542	1.5291	-0.5749
16	5d	0.0019	1.2683	1.2517	0.0166
17	7a	0.0139	2.1427	2.4534	-0.3107
18	7b	0.0057	1.7590	2.4045	-0.6455

q ²	r ²	SEP	SEE	N	F	r ² _{pred}	Fraction steric	electrostatic
0.767	0.961	0.337	0.138	2	81.544	0.837	0.672	0.328

q²: Leave-One-Out cross-validated correlation coefficient. r²: non-cross-validated correlation coefficient. SEP: standard error of prediction. SEE: standard error of estimate. N: optimum number of components. F: F-test value. r²_{pred}: predictive r².

0.337; SEE, 0.138 (Table 2). The corresponding field contributions of steric and electrostatic effects were 67% and 33%, respectively. Compared with the electrostatic field, the effect of the steric field on the predicted CSPs was greater than 2-fold. As an external validation, the test set was not included in building the CoMFA model, and the predictive ability of the model was also calculated, giving rise to a predictive r² (r²_{pred}) value of 0.837. Figure 3A shows plots of the actual versus predicted log(CSP) + 4 values of each molecule in the training and test sets of the CoMFA model. The blue and red circles indicate molecules in the training and test sets, respectively. The dashed line is the line of unity, where both the training and test set compounds are close enough to the line and show a linear relationship. The results of the analysis are represented by contour maps (Figure 3B–3D), showing favorable and unfavorable steric and electrostatic regions. All of the contours showed the contributions from favorable (green) and unfavorable (yellow) steric regions, as well as favorable electropositive (blue) and electronegative (red) substituents. These contour maps provided insight into the key structural features contributing to the binding activity of IL-33.

Within the training set, the series of compounds with the 2-(dimethylamino)ethyl substituent (**6a–6e** and **7c–7e**) had higher actual and predicted log(CSP) + 4 values (>2.0) than that of compound **5e** (1.5094). Contour maps of the initial hit compound **5e** and the most accurately predicted molecule **6c** with the lowest residual error of 0.0085 are shown in Figures 3 C and 3D,

respectively. As shown in Figure 3C, compound **5e** was located in the middle of the contours and did not occupy either a favorable or unfavorable region. On the other hand, compound **6c** occupied the sterically-favored region with bulky chains and the electro-negative region with negatively-charged atoms on the side chain (Figure 3D).

Cell-based assay of IL-6 production

Among the eighteen compounds evaluated in the 2D NMR studies, six compounds (**6a**, **6b**, **6c**, **6e**, **7c**, and **7e**) having actual and predicted log(CSP) + 4 values higher than 2.30 were selected for evaluation of IL-33 inhibition using a cell-based ELISA assay. Human mast cell line-1 (HMC-1) cells that produce IL-6 upon stimulation with IL-33 were treated with or without the selected compounds for 24 h at 37 °C. The cells treated with media or IL-33 only served as negative and positive controls, respectively. The amount of secreted IL-6 due to the stimulation of IL-33/ST2 signaling pathway was measured by ELISA. Of the six inhibitors, the *O*-alkylated compound **7c** inhibited IL-6 production in a dose-dependent manner (Figure 4). This significant inhibition of IL-6 production started at the inhibitor concentration of 0.03 μM and a maximal inhibition of 97.2% was achieved at a concentration of >0.3 μM. However, the other *O*-alkylated compound **7e** provided

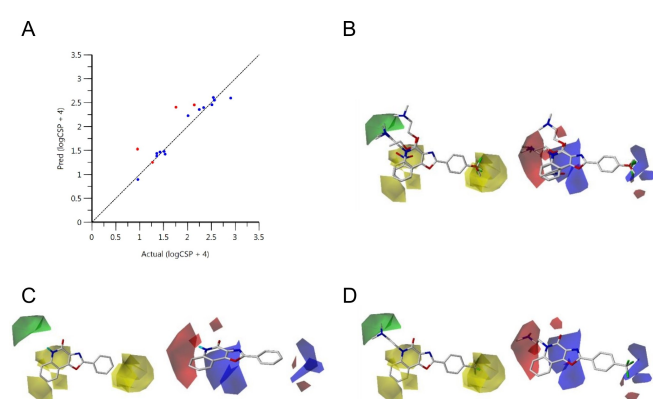


Figure 3. (A) Comparison of actual and predicted log(CSP) + 4 values from the CoMFA model. (B) CoMFA contour map with the aligned molecules of the training set. (C) CoMFA contour map with **5e**. (D) CoMFA contour map with the most accurately predicted molecule **6c**. Green contours indicate the regions where substitution of the bulky group enhances the binding affinity, while yellow contours indicate reduction of the binding affinity by the bulky group. Red contours indicate the regions where the electro-negative substituents enhance the binding affinity, and blue contours indicate where the electropositive substituents enhance the binding affinity.

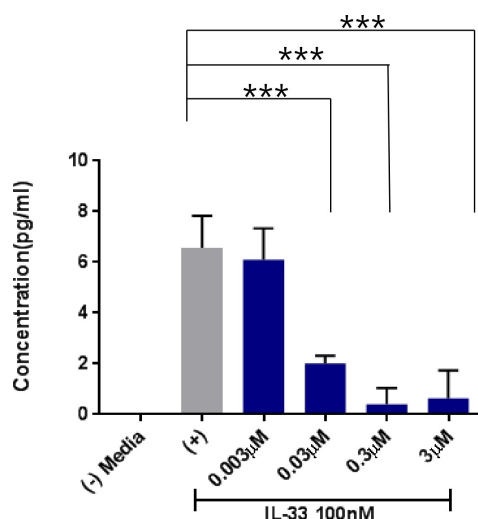


Figure 4. Inhibition of IL-6 production by compound **7c** in HMC-1 cells. Cells were treated with a mixture of IL-33 (100 nM) and compound **7c** at the indicated doses for 24 hr. Cells treated with media or IL-33 only served as negative and positive controls, respectively. These data are representative of three independent experiments. (***) $p < 0.005$

only ~30% inhibition at 3 μM (See supplementary data). Three *N*-alkylated products (**6a**, **6b** and **6c**) showed weak inhibition of IL-6 production, while compound **6e** was inactive even at 10 μM (See supplementary data).

Conclusion

IL-33 is one of alarmin cytokines in asthma and allergic response and plays a key role in recruiting eosinophils. Based on the chemical structure of BTB 11086, oxazolo[4,5-*c*]-quinolinone analogs were designed and synthesized as new IL-33 inhibitors. 2D-NMR analysis showed that most of the synthesized compounds interacted with the hot-spot amino acid residues of IL-33 more strongly than BTB11086, indicating that they might block the interaction between IL-33 and ST2. The most potent compound **7c** in this series inhibited the production of IL-6 stimulated by IL-33 with a maximal inhibition of 97.2% at $>0.3 \mu\text{M}$. Compound **7c** is the first small-molecule IL-33 inhibitor and could be used as a hit compound for the development of effective low molecular weight IL-33 inhibitors.

Experimental Section

General

All chemicals and solvents used in the reaction were purchased from Sigma-Aldrich and Organics and were used without further purification. Reaction progress was monitored by TLC on pre-coated silica gel plates with silica gel 60F₂₅₄ (Merck; Darmstadt, Germany) and visualized by UV254 light. Column chromatography was performed on silica gel (Silica gel 60; 230–400 mesh ASTM, Merck, Darmstadt, Germany). Nuclear magnetic resonance (NMR) spectra were recorded at room temperature on either a Bruker BioSpin Avance 300 MHz NMR (¹H, 300 MHz; ¹³C, 75 MHz) or a Bruker Ultrashield 600 MHz Plus (¹H, 600 MHz; ¹³C, 125 MHz) spectrometer. All chemical shifts are reported in parts per million (ppm) from tetramethylsilane ($\delta=0$) and were measured relative to the solvent in which the sample was analyzed (CDCl₃: δ 7.26 for ¹H NMR, δ 77.0 for ¹³C NMR; DMSO-*d*₆: δ 2.50 for ¹H NMR, δ 39.50 for ¹³C NMR). The ¹H NMR shift values are reported as chemical shift (δ), the corresponding integral, multiplicity (*s*=singlet, broad *s*=bs, *d*=doublet, *t*=triplet, *q*=quartet, *m*=multiplet, *dd*=doublet of doublets, *td*=triplet of doublets, *qd*=quartet of doublets), coupling constant (*J* in Hz) and assignments. Low resolution mass spectra (LRMS) were obtained on an Agilent 6460 Triple Quad LC/MS spectrometer and high resolution mass spectra (HRMS) were recorded on an Agilent 6530 Accurate Mass Q-TOF LC/MS spectrometer.

Ethyl 2-chlorooxazole-4-carboxylate (1)

Ethyl 2-aminooxazole-4-carboxylate (468 mg, 3 mmol) was added in portions to a solution of tert-butyl nitrite (540 μL , 0.45 mmol) and copper (II) chloride (600 mg, 4.5 mmol) in acetonitrile (22 mL) at 60 °C. The mixture was then stirred at 80 °C for 1 h. The mixture was cooled and partitioned between dichloromethane and iced water. The aqueous layer was further extracted with dichloromethane. The combined organic layer was washed with brine, dried (MgSO₄), and evaporated. The crude residue was purified by column chromatography on silica gel (eluting with hexane–Et₂O, 7:1 to 4:1, v/v) to afford compound **1** as white solid (338 mg, 64%). *R*_f=0.38 (hexane–Et₂O=2:1, v/v). ¹H NMR (300 MHz, CDCl₃) δ ppm 8.20 (*s*, 1H), 4.40 (*q*, *J*=7.2 Hz, 2H), 1.39 (*t*, *J*=

6.9 Hz, 3H). LRMS (ESI) *m/z* 176.1 [M+H]⁺. All spectroscopic data were in complete agreement with those reported previously.^[9]

Typical procedure of Suzuki coupling for the synthesis of ethyl 2-(4-fluorophenyl)oxazole-4-carboxylate (2a)

The ethyl 2-chlorooxazole-4-carboxylate **1** (257 mg, 1.47 mmol), 4-fluorophenylboronic acid (252 mg, 1.8 mmol, 1.2 eq), and tetrakis (triphenylphosphine) palladium (0) (85 mg, 0.07 mmol, 0.05 eq) were dissolved in toluene (20 mL) and 2 M potassium carbonate solution (2.0 mL, 4.0 mmol) at room temperature under nitrogen atmosphere. The reaction mixture was stirred under reflux for 1 h. After being cooled at room temperature, the reaction mixture and partitioned between ethyl acetate and 2 M sodium hydroxide solution. The aqueous layer was further washed with ethyl acetate twice. The combined organic layer was washed with brine, dried (MgSO₄), and concentrated in vacuo. The crude products were purified by column chromatography on silica gel (eluting with hexane–Et₂O, 5:1 to 3:1, v/v) to afford pure compound **2a** as white solid (250 mg, 73%). *R*_f=0.30 (hexane–Et₂O=2:1, v/v). ¹H NMR (300 MHz, CDCl₃) δ ppm 8.25 (*s*, 1H), 8.11 (*dd*, *J*=5.4 and 8.9 Hz, 2H), 7.16 (*t*, *J*=9.0 Hz, 2H), 4.42 (*q*, *J*=7.2 Hz, 2H), 1.40 (*t*, *J*=7.2 Hz, 3H); ¹³C NMR (75 MHz, CDCl₃) δ ppm 166.2, 162.9, 161.7, 161.3, 143.7, 134.7, 129.2, 129.1, 122.8, 122.8, 116.3, 116.1, 116.0, 115.7, 61.4, 14.3. LRMS (ESI) *m/z* 257.8 [M+Na]⁺. HRMS (ESI) *m/z* calculated for C₁₂H₁₀FNO₃Na⁺ [M+Na]⁺: 258.0537; found: 258.0528. All spectroscopic data were in complete agreement with those reported.^[13]

Compounds **2b–2e** were prepared using a similar method as described for **2a**.

Ethyl 2-(4-chlorophenyl)oxazole-4-carboxylate (2b)

This compound was obtained in 90% yield as white solid, following the same procedure described for the synthesis of **2a** with 4-chlorophenylboronic acid instead of 4-trifluorophenylboronic acid. *R*_f=0.38 (hexane–Et₂O=2:1, v/v). ¹H NMR (300 MHz, CDCl₃) δ ppm 8.27 (*s*, 1H), 8.05 (*d*, *J*=8.4 Hz, 2H), 7.45 (*d*, *J*=7.2 Hz, 2H), 4.43 (*q*, *J*=7.2 Hz, 2H), 1.40 (*t*, *J*=7.2 Hz, 3H). LRMS (ESI) *m/z* 251.8 [M+H]⁺ and 273.8 [M+Na]⁺. All spectroscopic data are in complete agreement with those reported.^[13]

Ethyl 2-(4-(trifluoromethyl)phenyl)oxazole-4-carboxylate (2c)

This compound was obtained in 64% yield as white solid, following the same procedure described for the synthesis of **2a** with 4-(trifluoromethyl)phenylboronic acid instead of 4-trifluorophenylboronic acid. *R*_f=0.38 (hexane–Et₂O=2:1, v/v). ¹H NMR (300 MHz, CDCl₃) δ ppm 8.32 (*s*, 1H), 8.24 (*d*, *J*=8.1 Hz, 2H), 7.74 (*d*, *J*=8.1 Hz, 2H), 4.45 (*q*, *J*=7.2 Hz, 2H), 1.42 (*t*, *J*=7.2 Hz, 3H). LRMS (ESI) *m/z* 286.0 [M+H]⁺ and 308.1 [M+Na]⁺. All spectroscopic data are in complete agreement with those reported.^[14]

Ethyl 2-(4-methoxyphenyl)oxazole-4-carboxylate (2d)

This compound was obtained in 70% yield as white needle-like crystal, following the same procedure described for the synthesis of **2a** with 4-methoxyphenylboronic acid instead of 4-trifluorophenylboronic acid. *R*_f=0.13 (hexane–Et₂O=2:1, v/v). ¹H NMR (300 MHz, CDCl₃) δ ppm 8.24 (*s*, 1H), 8.06 (*d*, *J*=9.0 Hz, 2H), 6.98 (*d*, *J*=9.0 Hz, 2H), 4.43 (*q*, *J*=7.2 Hz, 2H), 1.42 (*t*, *J*=7.2 Hz, 3H). LRMS (ESI) *m/z* 247.7 [M+H]⁺ and 269.9 [M+Na]⁺. All spectroscopic data are in complete agreement with those reported.^[13]

Ethyl 2-phenyloxazole-4-carboxylate (2e)

This compound was obtained in 54% yield as white needle-like crystal, following the same procedure described for the synthesis of **2a** with phenylboronic acid instead of 4-trifluorophenylboronic acid. $R_f=0.30$ (hexane-Et₂O=2:1, v/v). ¹H NMR (300 MHz, CDCl₃) δ ppm 8.28 (s, 1H), 8.12 (dd, J=2.1 and 7.2 Hz, 2H), 7.16 (dd, J=1.8 and 5.3 Hz, 2H), 4.43 (q, J=7.2 Hz, 2H), 1.41 (t, J=7.2 Hz, 3H). LRMS (ESI) m/z 218.0 [M+H]⁺ and 239.9 [M+Na]⁺. All spectroscopic data are in complete agreement with those reported.^[9]

Typical procedure of Heck reaction for the synthesis of ethyl 2-(4-fluorophenyl)-5-(2-nitrophenyl)oxazole-4-carboxylate (3a)

A mixture of **2a** (192 mg, 0.8 mmol), 2-iodonitrobenzene (398 mg, 1.6 mmol, 2.0 eq), palladium acetate (11.2 mg, 0.05 mmol, 0.06 eq), triphenyl phosphine (21 mg, 0.08 mmol, 0.1 eq), cesium carbonate (651.6 mg, 2.0 mmol, 2.5 eq), and DMF (4 mL) was flushed with nitrogen and stirred at 140 °C for 3 h. The cooled mixture was diluted with ethyl acetate and washed with water, brine, dried (MgSO₄), and concentrated under reduced pressure. The crude residue was purified by column chromatography on silica gel (eluting with hexane-Et₂O, 5:1 to 1:1, v/v) to afford compound **3a** as yellow needle-like crystal (192 mg, 67%). $R_f=0.35$ (hexane-Et₂O=1:1, v/v). ¹H NMR (300 MHz, CDCl₃) δ ppm 8.20 (d, J=8.1 Hz, 1H), 8.14 (q, J=8.4 Hz, 1H), 8.18–8.09 (m, 1H), 7.83–7.65 (m, 3H), 7.19 (t, J=8.7 Hz, 2H), 4.34 (q, J=7.2 Hz, 2H), 1.29 (t, J=7.2 Hz, 3H); ¹³C NMR (75 MHz, CDCl₃) δ ppm 166.3, 161.3, 160.6, 151.0, 148.5, 132.9, 132.6, 131.3, 130.2, 129.3, 129.2, 124.9, 122.6, 122.5, 122.5, 116.3, 116.0, 61.6, 14.0. LRMS (ESI) m/z 357.4 [M+H]⁺, 379.0 [M+Na]⁺, and 395.0 [M+K]⁺. HRMS (ESI) m/z calculated for C₁₈H₁₄FN₂O₅⁺ [M+H]⁺: 357.0881; found: 357.0865.

Compounds **3b–3e** were prepared using a similar method as described for **3a**.

Ethyl 2-(4-chlorophenyl)-5-(2-nitrophenyl)oxazole-4-carboxylate (3b)

This compound was obtained in 47% yield as white needle-like crystal, following the same procedure described for the synthesis of **3a**. $R_f=0.30$ (hexane-Et₂O=1:1, v/v). ¹H NMR (300 MHz, CDCl₃) δ ppm 8.18 (d, J=8.1 Hz, 1H), 8.05 (dd, J=4.2 and 10.1 Hz, 1H), 8.05 (d, J=8.7 Hz, 1H), 7.81–7.65 (m, 3H), 7.46 (d, J=8.7 Hz, 1H), 7.46 (dd, J=4.2 and 9.3 Hz, 1H), 4.31 (q, J=7.2 Hz, 2H), 1.26 (t, J=7.2 Hz, 3H); ¹³C NMR (75 MHz, CDCl₃) δ ppm 161.2, 160.5, 151.1, 148.5, 137.6, 132.8, 132.6, 131.3, 130.3, 129.2, 128.6, 124.9, 124.6, 122.6, 61.6, 29.7, 14.0. LRMS (ESI) m/z 373.1 [M+H]⁺, 395.0 [M+Na]⁺, and 411.0 [M+K]⁺. HRMS (ESI) m/z calculated for C₁₈H₁₄ClN₂O₅⁺ [M+H]⁺: 373.0586; found: 373.0589.

Ethyl 5-(2-nitrophenyl)-2-(4-(trifluoromethyl)phenyl)oxazole-4-carboxylate (3c)

This compound was obtained in 44% yield as white needle-like crystal, following the same procedure described for the synthesis of **3a**. $R_f=0.20$ (hexane-Et₂O=1:1, v/v). ¹H NMR (300 MHz, CDCl₃) δ ppm 8.24 (d, J=8.1 Hz, 2H), 8.21 (d, J=10.5 Hz, 1H), 7.86–7.68 (m, 5H), 4.32 (q, J=7.2 Hz, 2H), 1.27 (t, J=7.2 Hz, 3H); ¹³C NMR (75 MHz, CDCl₃) δ ppm 166.1, 159.9, 151.7, 148.5, 133.0, 132.6, 127.3, 126.0, 125.9, 124.9, 61.8, 14.0. LRMS (ESI) m/z 407.0 [M+H]⁺, 428.7 [M+Na]⁺, and 445.3 [M+K]⁺. HRMS (ESI) m/z calculated for C₁₈H₁₄F₃N₂O₅⁺ [M+H]⁺: 407.0849; found: 407.0809.

Ethyl 2-(4-methoxyphenyl)-5-(2-nitrophenyl)oxazole-4-carboxylate (3d)

This compound was obtained in 32% yield as white needle-like crystal, following the same procedure described for the synthesis of **3a**. $R_f=0.20$ (hexane-Et₂O=1:1, v/v). ¹H NMR (300 MHz, CDCl₃) δ ppm 8.18 (d, J=8.7 Hz, 1H), 8.07 (d, J=8.7 Hz, 2H), 7.82–7.64 (m, 3H), 7.00 (t, J=9.0 Hz, 2H), 4.33 (q, J=7.2 Hz, 2H), 1.28 (t, J=7.2 Hz, 3H); ¹³C NMR (75 MHz, CDCl₃) δ ppm 162.1, 161.5, 161.5, 150.4, 148.5, 132.8, 132.6, 131.1, 130.0, 128.8, 124.8, 122.8, 118.8, 114.3, 61.5, 55.5, 29.7, 14.1. LRMS (ESI) m/z 369.1 [M+H]⁺, 391.1 [M+Na]⁺, and 407.1 [M+K]⁺. HRMS (ESI) m/z calculated for C₁₉H₁₇N₂O₆⁺ [M+H]⁺: 369.1081; found: 369.1090.

Ethyl 5-(2-nitrophenyl)-2-phenyloxazole-4-carboxylate (3e)

This compound was obtained in 45% yield as white needle-like crystal, following the same procedure described for the synthesis of **3a**. $R_f=0.23$ (hexane-Et₂O=1:1, v/v). ¹H NMR (300 MHz, CDCl₃) δ ppm 8.19 (d, J=7.8 Hz, 1H), 8.16–8.08 (m, 1H), 8.12 (d, J=7.8 Hz, 1H), 7.76–7.66 (m, 1H), 7.77 (d, J=4.2 Hz, 2H), 7.55–7.43 (m, 3H), 4.32 (q, J=7.2 Hz, 2H), 1.27 (t, J=7.2 Hz, 3H). LRMS (ESI) m/z 339.3 [M+H]⁺, 361.1 [M+Na]⁺, and 377.0 [M+K]⁺. HRMS (ESI) m/z calculated for C₁₈H₁₄N₂O₅Na⁺ [M+Na]⁺: 361.0795; found: 361.0778. All spectroscopic data are in complete agreement with those reported.^[9]

Typical procedure of hydrogenation reaction for the synthesis of ethyl 5-(2-aminophenyl)-2-(4-fluorophenyl)oxazole-4-carboxylate (4a)

To a solution of **3a** (192 mg, 0.54 mmol) in MeOH (15 mL) was added catalytic amount of 10 wt. % palladium on activated carbon. The mixture was shaken under H₂ (50 psi) for 1 h. The reaction mixture was filtered through Celite bed. The filtrate was concentrated under reduced pressure to give **4a** (145 mg, 82%) as yellow solid. $R_f=0.30$ (hexane-Et₂O=1:1, v/v). ¹H NMR (300 MHz, CDCl₃) δ ppm 8.18–8.07 (m, 1H), 8.12 (q, J=8.4 Hz, 1H), 7.43 (dd, J=1.2 and 7.8 Hz, 1H), 7.29 (td, J=8.1 and 1.5 Hz, 1H), 7.22–7.08 (m, 1H), 7.16 (t, J=8.4 Hz, 1H), 6.84 (td, J=7.8 and 1.2 Hz, 1H), 6.82 (d, J=8.1 Hz, 1H), 4.39 (q, J=7.2 Hz, 2H), 4.16 (bs, 2H), 1.34 (t, J=7.2 Hz, 3H); ¹³C NMR (75 MHz, CDCl₃) δ ppm 166.2, 162.8, 162.1, 159.8, 154.4, 145.7, 131.8, 131.6, 129.8, 129.1, 129.0, 122.8, 122.8, 118.2, 116.7, 116.3, 116.0, 112.7, 61.5, 14.2. LRMS (ESI) m/z 327.1 [M+H]⁺ and 349.1 [M+Na]⁺. HRMS (ESI) m/z calculated for C₁₈H₁₆FN₂O₃⁺ [M+H]⁺: 327.1139; found: 327.1133.

Compounds **4b–4e** were prepared using a similar method as described for **4a**.

Ethyl 5-(2-aminophenyl)-2-(4-chlorophenyl)oxazole-4-carboxylate (4b)

This compound was obtained in 87% yield as white needle-like crystal, following the same procedure described for the synthesis of **4a**. $R_f=0.23$ (hexane-Et₂O=1:1, v/v). ¹H NMR (300 MHz, CDCl₃) δ ppm 8.20 (d, J=8.1 Hz, 1H), 8.14 (dd, J=5.4 and 8.9 Hz, 2H), 7.83–7.65 (m, 3H), 7.19 (t, J=8.7 Hz, 2H), 4.44 (q, J=7.2 Hz, 2H), 1.29 (t, J=7.2 Hz, 3H); ¹³C NMR (75 MHz, CDCl₃) δ ppm 166.3, 161.3, 160.6, 151.0, 148.5, 132.9, 132.6, 131.3, 130.2, 129.3, 129.2, 124.9, 122.6, 122.5, 116.3, 116.0, 61.6, 14.0. LRMS (ESI) m/z 343.1 [M+H]⁺, 365.1 [M+Na]⁺. HRMS (ESI) m/z calculated for C₁₈H₁₅ClN₂O₃Na⁺ [M+Na]⁺: 365.0663; found: 365.0678

Ethyl 5-(2-aminophenyl)-2-(4-(trifluoromethyl)phenyl)oxazole-4-carboxylate (4c)

This compound was obtained in 98% yield as white needle-like crystal, following the same procedure described for the synthesis of **4a**. $R_f = 0.29$ (CH_2Cl_2 -MeOH = 20:1, v/v). $^1\text{H NMR}$ (300 MHz, CDCl_3) δ ppm 8.25 (d, $J = 8.1$ Hz, 2H), 7.74 (d, $J = 8.1$ Hz, 2H), 7.44 (t, $J = 7.8$ Hz, 1H), 7.31 (t, $J = 7.8$ Hz, 1H), 6.86 (t, $J = 7.5$ Hz, 1H), 6.83 (d, $J = 7.8$ Hz, 1H), 4.40 (q, $J = 7.2$ Hz, 2H), 4.17 (s, 2H), 1.29 (t, $J = 7.2$ Hz, 3H); $^{13}\text{C NMR}$ (75 MHz, CDCl_3) δ ppm 162.0, 159.2, 155.1, 132.0, 131.6, 127.1, 126.0, 125.9, 118.2, 116.9, 112.4, 61.7, 14.2. LRMS (ESI) m/z 356.8 $[\text{M} + \text{H}]^+$ and 398.9 $[\text{M} + \text{Na}]^+$. HRMS (ESI) m/z calculated for $\text{C}_{18}\text{H}_{16}\text{F}_3\text{N}_2\text{O}_3^+$ $[\text{M} + \text{Na}]^+$: 377.1108; found: 377.1094.

Ethyl 5-(2-aminophenyl)-2-(4-methoxyphenyl)oxazole-4-carboxylate (4d)

This compound was obtained in 89% yield as white needle-like crystal, following the same procedure described for the synthesis of **4a**. $R_f = 0.28$ (CH_2Cl_2 -MeOH = 20:1, v/v). $^1\text{H NMR}$ (300 MHz, CDCl_3) δ ppm 8.07 (d, $J = 8.7$ Hz, 2H), 7.44 (d, $J = 7.5$ Hz, 1H), 7.28 (t, $J = 8.1$ Hz, 2H), 6.98 (d, $J = 8.7$ Hz, 1H), 6.85 (t, $J = 7.5$ Hz, 1H), 6.81 (d, $J = 7.8$ Hz, 1H), 4.39 (q, $J = 7.2$ Hz, 2H), 4.18 (bs, 2H), 1.34 (t, $J = 7.2$ Hz, 3H); $^{13}\text{C NMR}$ (75 MHz, CDCl_3) δ ppm 162.8, 162.3, 157.8, 151.9, 138.4, 130.2, 129.3, 122.7, 121.6, 119.1, 115.4, 114.4, 111.6, 61.4, 55.4, 14.2. LRMS (ESI) m/z 339.1 $[\text{M} + \text{H}]^+$ and 361.1 $[\text{M} + \text{Na}]^+$. HRMS (ESI) m/z calculated for $\text{C}_{19}\text{H}_{19}\text{N}_2\text{O}_4^+$ $[\text{M} + \text{H}]^+$: 339.1339; found: 339.1452.

Ethyl 5-(2-aminophenyl)-2-phenyloxazole-4-carboxylate (4e)

This compound was obtained in 70% yield as white needle-like crystal, following the same procedure described for the synthesis of **4a**. $R_f = 0.40$ (hexane-Et₂O = 1:2, v/v). $^1\text{H NMR}$ (300 MHz, CDCl_3) δ ppm 8.22–8.11 (m, 1H), 8.15 (d, $J = 7.8$ Hz, 1H), 7.54–7.41 (m, 4H), 7.31 (td, $J = 8.7$ and 1.5 Hz, 1H), 6.87 (t, $J = 7.5$ Hz, 1H), 6.84 (d, $J = 8.1$ Hz, 1H), 4.42 (q, $J = 7.2$ Hz, 2H), 4.25 (bs, 2H), 1.38 (t, $J = 7.2$ Hz, 3H). LRMS (ESI) m/z 309.3 $[\text{M} + \text{H}]^+$, 331.2 $[\text{M} + \text{Na}]^+$, and 347.0 $[\text{M} + \text{K}]^+$. HRMS (ESI) m/z calculated for $\text{C}_{18}\text{H}_{16}\text{N}_2\text{O}_3\text{Na}^+$ $[\text{M} + \text{Na}]^+$: 331.1053; found: 331.1051. All spectroscopic data are in complete agreement with those reported.^[9]

Typical procedure of cyclization reaction for the synthesis of 2-(4-fluorophenyl)oxazolo[4,5-c]quinolin-4(5H)-one (5a)

A mixture of **4a** (95 mg, 0.27 mmol), DME (7 mL), and 2 M potassium carbonate solution (0.5 mL, 1.0 mmol) was stirred under reflux for 12 h. The solvent was removed under reduced pressure and water added. The solid was collected by filtration, washed with cool EtOH, and dried in vacuo to give **5a** (45 mg, 60%). $R_f = 0.18$ (CH_2Cl_2 -MeOH = 1:1, v/v). $^1\text{H NMR}$ (300 MHz, $\text{DMSO}-d_6$) δ ppm 11.19 (bs, 1H), 7.40 (d, $J = 9.0$ Hz, 1H), 7.38 (d, $J = 9.0$ Hz, 1H), 7.14 (d, $J = 7.8$ Hz, 1H), 6.71 (t, $J = 7.2$ Hz, 1H), 6.35 (d, $J = 7.2$ Hz, 1H), 6.59 (d, $J = 8.7$ Hz, 1H), 6.47 (t, $J = 7.8$ Hz, 1H); $^{13}\text{C NMR}$ (75 MHz, CDCl_3) δ ppm 166.3, 161.3, 160.6, 151.0, 148.5, 132.9, 132.6, 131.3, 130.2, 129.3, 129.2, 124.9, 122.6, 122.5, 122.5, 116.3, 116.0, 61.6, 14.0. LRMS (ESI) m/z 302.7 $[\text{M} + \text{Na}]^+$ and 318.8 $[\text{M} + \text{K}]^+$. HRMS (ESI) m/z calculated for $\text{C}_{16}\text{H}_{10}\text{FN}_2\text{O}_2^+$ $[\text{M} + \text{H}]^+$: 281.0721; found: 281.0713.

Compounds **5b–5e** were prepared using a similar method as described for **5a**.

2-(4-Chlorophenyl)oxazolo[4,5-c]quinolin-4(5H)-one (5b)

This compound was obtained in 82% yield, following the same procedure described for the synthesis of **5a**. $R_f = 0.32$ (CH_2Cl_2 -MeOH = 20:1, v/v). $^1\text{H NMR}$ (300 MHz, $\text{DMSO}-d_6$) δ ppm 8.24 (d, $J = 8.4$ Hz, 2H), 8.01 (d, $J = 7.5$ Hz, 1H), 7.02 (t, $J = 8.7$ Hz, 2H), 7.56 (d, $J = 7.5$ Hz, 1H), 7.51 (t, $J = 8.4$ Hz, 1H), 7.31 (t, $J = 7.5$ Hz, 1H); $^{13}\text{C NMR}$ (75 MHz, CDCl_3) δ ppm 166.3, 161.3, 160.6, 151.0, 148.5, 132.9, 132.6, 131.3, 130.2, 129.3, 129.2, 124.9, 122.6, 122.5, 122.5, 116.3, 116.0, 61.6, 14.0. LRMS (ESI) m/z 335.2 $[\text{M} + \text{K}]^+$. HRMS (ESI) m/z calculated for $\text{C}_{16}\text{H}_9\text{ClN}_2\text{O}_2\text{Na}^+$ $[\text{M} + \text{Na}]^+$: 319.0245; found: 319.0276.

2-(4-(Trifluoromethyl)phenyl)oxazolo[4,5-c]quinolin-4(5H)-one (5c)

This compound was obtained in 72% yield, following the same procedure described for the synthesis of **5a**. $R_f = 0.38$ (CH_2Cl_2 -MeOH = 20:1, v/v). $^1\text{H NMR}$ (300 MHz, $\text{DMSO}-d_6$) δ ppm 8.44 (d, $J = 8.1$ Hz, 2H), 8.08 (d, $J = 7.8$ Hz, 1H), 8.03 (d, $J = 8.4$ Hz, 2H), 7.63 (t, $J = 7.2$ Hz, 1H), 7.53 (d, $J = 8.1$ Hz, 1H), 7.38 (t, $J = 7.5$ Hz, 1H); $^{13}\text{C NMR}$ (75 MHz, CDCl_3) δ ppm 166.3, 161.3, 160.6, 151.0, 148.5, 132.9, 132.6, 131.3, 130.2, 129.3, 129.2, 124.9, 122.6, 122.5, 122.5, 116.3, 116.0, 61.6, 14.0. LRMS (ESI) m/z 353.5 $[\text{M} + \text{Na}]^+$ and 369.0 $[\text{M} + \text{K}]^+$. HRMS (ESI) m/z calculated for $\text{C}_{17}\text{H}_{10}\text{F}_3\text{N}_2\text{O}_2^+$ $[\text{M} + \text{H}]^+$: 331.0689; found: 331.0682.

2-(4-Methoxyphenyl)oxazolo[4,5-c]quinolin-4(5H)-one (5d)

This compound was obtained in 60% yield, following the same procedure described for the synthesis of **5a**. $R_f = 0.28$ (CH_2Cl_2 -MeOH = 20:1, v/v). $^1\text{H NMR}$ (300 MHz, $\text{DMSO}-d_6$) δ ppm 11.18 (bs, 1H), 7.38–7.31 (m, 1H), 7.33 (d, $J = 9.0$ Hz, 1H), 7.19 (dd, $J = 1.2$ and 8.1 Hz, 1H), 6.76 (td, $J = 8.4$ and 1.5 Hz, 1H), 6.68 (d, $J = 9.0$ Hz, 1H), 6.53 (td, $J = 8.1$ and 1.2 Hz, 1H), 6.41–6.33 (m, 1H), 6.35 (d, $J = 9.0$ Hz, 1H); $^{13}\text{C NMR}$ (75 MHz, CDCl_3) δ ppm 166.3, 161.3, 160.6, 151.0, 148.5, 132.9, 132.6, 131.3, 130.2, 129.3, 129.2, 124.9, 122.6, 122.5, 122.5, 116.3, 116.0, 61.6, 14.0. LRMS (ESI) m/z 293.1 $[\text{M} + \text{H}]^+$, 314.9 $[\text{M} + \text{Na}]^+$, and 331.0 $[\text{M} + \text{K}]^+$. HRMS (ESI) m/z calculated for $\text{C}_{17}\text{H}_{13}\text{N}_2\text{O}_3^+$ $[\text{M} + \text{H}]^+$: 293.0921; found: 293.0919.

2-Phenyloxazolo[4,5-c]quinolin-4(5H)-one (5e)

This compound was obtained in 75% yield, following the same procedure described for the synthesis of **5a**. $R_f = 0.30$ (CH_2Cl_2 -MeOH = 20:1, v/v). $^1\text{H NMR}$ (300 MHz, $\text{DMSO}-d_6$) δ ppm 12.08 (bs, 1H), 8.29–8.18 (m, 2H), 8.05 (d, $J = 7.8$ Hz, 1H), 7.72–7.56 (m, 4H), 7.52 (d, $J = 8.1$ Hz, 1H), 7.37 (t, $J = 7.8$ Hz, 1H); $^{13}\text{C NMR}$ (75 MHz, CDCl_3) δ ppm 166.3, 161.3, 160.6, 151.0, 148.5, 132.9, 132.6, 131.3, 130.2, 129.3, 129.2, 124.9, 122.6, 122.5, 122.5, 116.3, 116.0, 61.6, 14.0. LRMS (ESI) m/z 262.8 $[\text{M} + \text{H}]^+$, 285.2 $[\text{M} + \text{Na}]^+$, and 300.6 $[\text{M} + \text{K}]^+$. HRMS (ESI) m/z calculated for $\text{C}_{16}\text{H}_{11}\text{N}_2\text{O}_2^+$ $[\text{M} + \text{H}]^+$: 263.0815; found: 263.0845. All spectroscopic data are in complete agreement with those reported.^[9]

General procedure of N- and O-alkylation for the synthesis of compounds (6a–8e)

A slurry of **5a** (43 mg, 0.153 mmol), 2-bromo-N,N-dimethylethanamine hydrobromide (80 mg, 0.31 mmol, 1.2 eq), and potassium carbonate (63 mg, 0.46 mmol, 3.0 eq) in DMF (5 mL) was stirred at 130 °C for 3 h and allowed to cool to room temperature. The solvent was removed under reduced pressure. Purification on silica gel column chromatography with Et₂O-MeOH, 10:1 to 3:1, v/v

v as the eluent afforded **6a** (21 mg, 39%), **7a** (9 mg, 17%), and **8a** (13 mg, 29%).

6a $R_f=0.15$ (Et₂O–MeOH=5:1, v/v). ¹H NMR (300 MHz, CDCl₃) δ ppm 8.33–8.22 (m, 1H), 8.29 (dd, J=5.4 and 8.7 Hz, 1H), 8.03 (dd, J=1.5 and 8.0 Hz, 1H), 7.64 (td, J=7.2 and 1.2 Hz, 1H), 7.57 (d, J=8.4 Hz, 1H), 7.38 (t, J=6.9 Hz, 1H), 7.22 (t, J=8.4 Hz, 1H), 7.27–7.16 (m, 1H), 4.58 (t, J=7.8 Hz, 2H), 2.66 (t, J=7.8 Hz, 2H), 2.41 (s, 6H); ¹³C NMR (75 MHz, CDCl₃) δ ppm 166.5, 163.1, 161.7, 157.3, 152.3, 130.5, 129.8, 129.7, 129.6, 122.8, 122.8, 121.9, 116.4, 116.1, 115.4, 111.6, 56.3, 45.9, 40.8, 29.7, 22.7. LRMS (ESI) m/z 352.2 [M+H]⁺ and 374.0 [M+Na]⁺. HRMS (ESI) m/z calculated for C₁₈H₁₉FN₃O₂⁺ [M+H]⁺: 352.1456; found: 352.1496.

7a $R_f=0.30$ (Et₂O–MeOH=5:1, v/v). ¹H NMR (300 MHz, CDCl₃) δ ppm 8.41–8.28 (m, 1H), 8.29 (dd, J=5.4 and 9.0 Hz, 1H), 8.14 (d, J=8.1 Hz, 1H), 7.96 (d, J=8.1 Hz, 1H), 7.67 (ddd, J=1.5, 7.1, and 8.4 Hz, 1H), 7.52 (td, J=8.0 and 0.9 Hz, 1H), 7.29–7.18 (m, 2H), 4.83 (t, J=6.0 Hz, 2H), 2.93 (t, J=6.0 Hz, 2H), 2.41 (s, 6H); ¹³C NMR (75 MHz, CDCl₃) δ ppm 166.6, 163.2, 161.8, 154.6, 153.9, 144.2, 129.9, 129.8, 128.0, 126.4, 124.8, 123.0, 123.0, 120.2, 116.4, 116.1, 114.6, 64.1, 57.9, 45.8, 29.7. LRMS (ESI) m/z 352.2 [M+H]⁺ and 374.0 [M+Na]⁺. HRMS (ESI) m/z calculated for C₂₀H₁₉FN₃O₂⁺ [M+H]⁺: 352.1456; found: 352.1498.

8a $R_f=0.93$ (Et₂O–MeOH=5:1, v/v). ¹H NMR (300 MHz, CDCl₃) δ ppm 8.31 (dd, J=5.1 and 8.9 Hz, 1H), 8.31 (t, J=5.0 Hz, 1H), 8.03 (dd, J=1.2 and 7.9 Hz, 1H), 7.64 (t, J=8.7 Hz, 1H), 7.52 (d, J=8.4 Hz, 1H), 7.39 (dd, J=5.4 and 9.0 Hz, 1H), 7.22 (t, J=8.4 Hz, 1H), 3.86 (s, 3H); ¹³C NMR (75 MHz, CDCl₃) δ ppm 166.5, 163.1, 161.7, 157.7, 138.5, 130.5, 130.0, 129.7, 129.6, 122.8, 121.7, 121.6, 116.4, 116.1, 115.4, 111.4, 29.9. LRMS (ESI) m/z 295.2 [M+H]⁺ and 317.0 [M+Na]⁺. HRMS (ESI) m/z calculated for C₁₇H₁₁FN₂O₂Na⁺ [M+Na]⁺: 317.0697; found: 317.0745.

Compounds **6b**, **7b** and **8b** were obtained by using **5b** instead of **5a** by following the same procedure described for the synthesis of **6a–8a**.

6b Yield: 26%. $R_f=0.17$ (Et₂O–MeOH=5:1, v/v). ¹H NMR (300 MHz, CDCl₃) δ ppm 8.24 (d, J=8.7 Hz, 2H), 8.04 (d, J=8.1 Hz, 1H), 7.96 (d, J=8.4 Hz, 1H), 7.68 (td, J=7.5 and 1.5 Hz, 1H), 7.53 (d, J=8.7 Hz, 2H), 7.42 (t, J=7.8 Hz, 1H), 4.43 (t, J=5.1 Hz, 2H), 2.86 (t, J=5.1 Hz, 2H), 2.41 (s, 6H); ¹³C NMR (75 MHz, CDCl₃) δ ppm 151.6, 138.1, 136.9, 130.6, 129.4, 129.0, 128.7, 127.5, 123.5, 121.44, 113.7, 109.5, 57.3, 53.4, 45.8, 29.7. LRMS (ESI) m/z 368.0 [M+H]⁺ and 390.2 [M+Na]⁺. HRMS (ESI) m/z calculated for C₂₀H₁₉ClN₃O₂⁺ [M+H]⁺: 368.1160; found: 368.1202.

7b Yield: 8%. $R_f=0.28$ (Et₂O–MeOH=5:1, v/v). ¹H NMR (300 MHz, CDCl₃) δ ppm 8.27 (d, J=8.4 Hz, 2H), 8.14 (d, J=8.1 Hz, 1H), 7.96 (d, J=8.1 Hz, 1H), 7.67 (t, J=7.5 Hz, 1H), 7.53 (d, J=8.1 Hz, 3H), 4.84 (t, J=5.1 Hz, 2H), 2.94 (t, J=5.1 Hz, 2H), 2.42 (s, 6H); ¹³C NMR (75 MHz, CDCl₃) δ ppm 161.7, 154.6, 153.9, 144.3, 138.0, 129.4, 129.3, 128.4, 128.0, 126.4, 125.2, 124.8, 120.2, 114.6, 64.8, 57.9, 53.4, 45.8, 31.9. LRMS (ESI) m/z 368.2 [M+H]⁺ and 390.2 [M+Na]⁺. HRMS (ESI) m/z calculated for C₂₀H₁₉ClN₃O₂⁺ [M+H]⁺: 368.1160; found: 368.1195.

8b Yield: 22%. $R_f=0.91$ (Et₂O–MeOH=5:1, v/v). ¹H NMR (300 MHz, CD₃CD) δ ppm 8.27 (d, J=8.7 Hz, 2H), 8.10 (d, J=8.1 Hz, 1H), 7.69–7.61 (m, 3H), 7.54 (d, J=7.8 Hz, 1H), 7.44 (d, J=7.5 Hz, 1H), 3.21 (s, 3H); LRMS (ESI) m/z 311.2 [M+H]⁺ and 333.1 [M+Na]⁺. HRMS (ESI) m/z calculated for C₁₇H₁₁ClN₂O₂Na⁺ [M+Na]⁺: 333.0401; found: 333.0406.

Compounds **6c**, **7c** and **8c** were obtained by using **5c** instead of **5a** by following the same procedure described for the synthesis of **6a–8a**.

6c Yield: 37%. $R_f=0.13$ (Et₂O–MeOH=5:1, v/v). ¹H NMR (300 MHz, CDCl₃) δ ppm 8.43 (d, J=8.1 Hz, 2H), 8.09 (dd, J=1.2 and 7.8 Hz, 1H), 7.81 (d, J=8.4 Hz, 2H), 7.68 (dddd, J=1.5, 7.2, and 8.7 Hz, 1H), 7.60 (d, J=8.4 Hz, 1H), 7.41 (td, J=7.8 and 0.9 Hz, 1H), 4.60 (t, J=7.5 Hz, 2H), 2.68 (t, J=7.8 Hz, 2H), 2.42 (s, 6H); ¹³C NMR (75 MHz, CDCl₃) δ ppm 161.0, 157.3, 152.8, 138.1, 131.0, 127.7, 126.1, 126.1, 126.0, 122.8, 122.1, 115.5, 111.5, 56.3, 45.9, 37.6. LRMS (ESI) m/z 402.1 [M+H]⁺ and 424.1 [M+Na]⁺. HRMS (ESI) m/z calculated for C₂₁H₁₉F₃N₃O₂⁺ [M+H]⁺: 402.1424; found: 402.1426.

7c Yield: 10%. $R_f=0.38$ (Et₂O–MeOH=5:1, v/v). ¹H NMR (300 MHz, CDCl₃) δ ppm 8.47 (d, J=8.1 Hz, 2H), 8.18 (d, J=7.8 Hz, 1H), 7.98 (d, J=8.4 Hz, 1H), 7.82 (d, J=8.4 Hz, 2H), 7.69 (td, J=7.2 and 1.5 Hz, 1H), 7.54 (td, J=7.2 and 1.2 Hz, 1H), 4.49 (t, J=6.3 Hz, 2H), 2.94 (t, J=6.0 Hz, 2H), 2.42 (s, 6H); ¹³C NMR (75 MHz, CDCl₃) δ ppm 166.1, 154.7, 154.1, 144.4, 129.8, 129.5, 128.0, 127.8, 126.4, 126.0, 126.0, 124.9, 120.4, 114.5, 64.2, 59.6, 45.9. LRMS (ESI) m/z 402.1 [M+H]⁺ and 424.1 [M+Na]⁺. HRMS (ESI) m/z calculated for C₂₁H₁₉F₃N₃O₂⁺ [M+H]⁺: 402.1424; found: 402.1437.

8c Yield: 32%. $R_f=0.88$ (Et₂O–MeOH=5:1, v/v). ¹H NMR (300 MHz, CDCl₃) δ ppm 8.43 (d, J=8.1 Hz, 2H), 8.07 (dd, J=1.2 and 7.8 Hz, 1H), 7.81 (d, J=8.7 Hz, 2H), 7.68 (dddd, J=1.5, 7.2, and 8.7 Hz, 1H), 7.54 (d, J=8.4 Hz, 1H), 7.42 (t, J=7.8 Hz, 1H), 3.87 (s, 6H); ¹³C NMR (75 MHz, CDCl₃) δ ppm 161.0, 157.6, 153.1, 138.8, 130.9, 127.7, 126.0, 126.0, 122.9, 121.9, 121.8, 115.5, 111.2, 29.4. LRMS (ESI) m/z 345.1 [M+H]⁺ and 367.1 [M+Na]⁺. HRMS (ESI) m/z calculated for C₁₈H₁₂F₃N₂O₂⁺ [M+H]⁺: 345.0845; found: 345.0842.

Compounds **6d**, **7d** and **8d** were obtained by using **5d** instead of **5a** by following the same procedure described for the synthesis of **6a–8a**.

6d Yield: 18%. $R_f=0.08$ (Et₂O–MeOH=5:1, v/v). ¹H NMR (300 MHz, CDCl₃) δ ppm 8.24 (d, J=9.0 Hz, 2H), 8.04 (d, J=8.4 Hz, 1H), 7.64–7.60 (m, 2H), 7.40–7.33 (m, 1H), 7.04 (d, J=8.7 Hz, 2H), 4.62 (t, J=7.5 Hz, 2H), 3.09 (s, 3H), 2.72 (t, J=7.8 Hz, 2H), 2.44 (s, 6H); ¹³C NMR (75 MHz, CDCl₃) δ ppm 162.8, 162.4, 157.5, 152.0, 137.6, 130.1, 129.9, 129.4, 122.6, 121.8, 119.1, 115.4, 114.4, 111.8, 56.0, 55.5, 45.6, 40.5, 29.7. LRMS (ESI) m/z 364.1 [M+H]⁺ and 387.1 [M+Na]⁺. HRMS (ESI) m/z calculated for C₂₁H₂₂N₃O₃⁺ [M+H]⁺: 364.1656; found: 364.1694.

7d Yield: 15%. $R_f=0.18$ (Et₂O–MeOH=5:1, v/v). ¹H NMR (300 MHz, CDCl₃) δ ppm 8.26 (d, J=8.1 Hz, 2H), 8.16 (d, J=6.3 Hz, 1H), 7.96 (d, J=8.4 Hz, 1H), 7.66 (dd, J=6.9 and 14.3 Hz, 1H), 7.54 (dd, J=7.8 and 16.2 Hz, 1H), 7.05 (d, J=8.7 Hz, 2H), 4.86 (t, J=6.3 Hz, 2H), 3.91 (s, 3H), 3.01 (t, J=6.3 Hz, 2H), 2.47 (s, 6H); ¹³C NMR (75 MHz, CDCl₃) δ ppm 163.0, 162.5, 154.6, 153.6, 144.0, 129.4, 128.8, 127.9, 126.5, 124.7, 120.2, 119.2, 114.8, 114.5, 63.7, 57.8, 55.5, 45.6, 30.4. LRMS (ESI) m/z 364.5 [M+H]⁺ and 387.5 [M+Na]⁺. HRMS (ESI) m/z calculated for C₂₁H₂₂N₃O₃⁺ [M+H]⁺: 364.1656; found: 364.1693.

8d Yield: 27%. $R_f=0.83$ (Et₂O–MeOH=5:1, v/v). ¹H NMR (300 MHz, CDCl₃) δ ppm 8.26 (d, J=8.7 Hz, 2H), 8.05 (d, J=7.8 Hz, 1H), 7.64 (t, J=8.7 Hz, 1H), 7.53 (d, J=8.4 Hz, 1H), 7.39 (t, J=7.8 Hz, 1H), 7.04 (d, J=9.0 Hz, 2H), 3.91 (s, 3H), 3.87 (s, 3H); ¹³C NMR (75 MHz, CDCl₃) δ ppm 162.8, 162.3, 157.8, 151.9, 138.4, 130.2, 130.1, 129.3, 122.7, 121.6, 119.1, 115.4, 114.4, 111.6, 55.5, 29.7, 29.4. LRMS (ESI) m/z 306.9 [M+H]⁺ and 329.9 [M+Na]⁺. HRMS (ESI) m/z calculated for C₁₈H₁₅N₂O₃⁺ [M+H]⁺: 307.1077; found: 307.1104.

Compounds **6e**, **7e** and **8d** were obtained by using **5e** instead of **5a** by following the same procedure described for the synthesis of **6a–8a**.

6e Yield: 39%. $R_f=0.25$ (Et₂O–MeOH=5:1, v/v). ¹H NMR (300 MHz, CDCl₃) δ ppm 8.34–8.27 (m, 2H), 8.07 (dd, J=1.5 and 7.8 Hz, 1H), 7.69–7.51 (m, 5H), 7.38 (td, J=7.2 and 1.2 Hz, 1H), 4.59 (t, J=7.5 Hz, 2H), 2.68 (t, J=7.5 Hz, 2H), 2.41 (s, 6H); ¹³C NMR (75 MHz, CDCl₃) δ

ppm 162.6, 157.4, 152.3, 137.9, 131.6, 130.5, 130.0, 129.0, 127.4, 126.5, 122.6, 122.0, 115.4, 111.8, 56.3, 45.9, 40.9. LRMS (ESI) m/z 333.4 $[M+H]^+$ and 355.3 $[M+Na]^+$. HRMS (ESI) m/z calculated for $C_{20}H_{20}N_3O_2^+$ $[M+H]^+$: 334.1550; found: 334.1557.

7e Yield: 9%. $R_f=0.36$ (Et_2O - $MeOH=5:1$, v/v). 1H NMR (300 MHz, $CDCl_3$) δ ppm 8.38–8.31 (m, 2H), 8.16 (dd, $J=0.9$ and 8.1 Hz, 1H), 7.96 (d, $J=8.4$ Hz, 1H), 7.66 (td, $J=7.2$ and 1.5 Hz, 1H), 7.59–7.48 (m, 4H), 4.84 (t, $J=6.0$ Hz, 2H), 2.94 (t, $J=6.0$ Hz, 1H), 2.42 (s, 6H); ^{13}C NMR (75 MHz, $CDCl_3$) δ ppm 163.0, 154.7, 153.9, 144.2, 131.6, 129.1, 129.0, 127.9, 127.6, 126.7, 126.5, 124.7, 120.3, 114.7, 64.1, 57.9, 45.9. LRMS (ESI) m/z 333.9 $[M+H]^+$ and 356.9 $[M+Na]^+$. HRMS (ESI) m/z calculated for $C_{20}H_{20}N_3O_2^+$ $[M+H]^+$: 334.1550; found: 334.1552.

8e Yield: 3%. $R_f=0.84$ (Et_2O - $MeOH=5:1$, v/v). 1H NMR (300 MHz, $CDCl_3$) δ ppm 8.36–8.08 (m, 2H), 8.08 (dd, $J=1.5$ and 7.8 Hz, 1H), 7.64 (dd, $J=1.5$ and 7.8 Hz, 1H), 7.59–7.51 (m, 4H), 7.41 (td, $J=7.2$ and 0.9 Hz, 1H), 3.88 (s, 3H); ^{13}C NMR (75 MHz, $CDCl_3$) δ ppm 131.6, 130.5, 129.0, 127.5, 126.5, 122.7, 121.8, 115.4, 111., 29.9, 29.7. LRMS (ESI) m/z 277.1 $[M+H]^+$ and 299.1 $[M+Na]^+$. HRMS (ESI) m/z calculated for $C_{17}H_{13}N_2O_2^+$ $[M+H]^+$: 277.0972; found: 277.0977.

General procedure of N- and O-alkylation for the synthesis of compounds 9a–9b

A slurry of **5a** (98 mg, 0.35 mmol), 2-bromo-*N,N*-diethylethanamine hydrobromide (456 mg, 1.75 mmol, 5.0 eq), and potassium carbonate (483 mg, 3.5 mmol, 10.0 eq) in DMF (7 mL) was stirred at 130 °C for 5 h and allowed to cool to room temperature. The excess solvent was removed under reduced pressure. Purification on silica gel column chromatography with Et_2O - $MeOH$, 20:1 to 5:1, v/v as the eluent afforded **9a** (18.6 mg, 14%) and **9b** (10.6 mg, 8%).

9a Yield: 14%. $R_f=0.39$ (Et_2O - $MeOH=5:1$, v/v). 1H NMR (300 MHz, $CDCl_3$) δ ppm 8.35–8.26 (m, 1H), 8.30 (dd, $J=5.4$ and 8.7 Hz, 1H), 8.03 (d, $J=7.5$ Hz, 1H), 7.66–7.59 (m, 2H), 7.43–7.34 (m, 1H), 7.22 (t, $J=8.7$ Hz, 2H), 4.55 (t, $J=7.8$ Hz, 2H), 2.79 (t, $J=7.8$ Hz, 2H), 2.68 (dd, $J=7.2$ and 14.4 Hz, 4H), 1.09 (t, $J=7.2$ Hz, 6H); ^{13}C NMR (75 MHz, $CDCl_3$) δ ppm 166.5, 163.2, 161.7, 157.4, 152.3, 138.0, 130.5, 129.8, 129.7, 129.6, 122.8, 122.8, 122.6, 121.8, 116.4, 116.1, 115.6, 111.6, 50.0, 47.6, 41.2, 12.0. LRMS (ESI) m/z 380.3 $[M+H]^+$. HRMS (ESI) m/z calculated for $C_{22}H_{23}FN_3O_2^+$ $[M+H]^+$: 380.1769; found: 380.1817.

9b Yield: 8%. $R_f=0.51$ (Et_2O - $MeOH=5:1$, v/v). 1H NMR (300 MHz, $CDCl_3$) δ ppm 8.38–8.31 (m, 1H), 8.35 (dd, $J=5.4$ and 9.0 Hz, 1H), 8.14 (d, $J=7.8$ Hz, 1H), 7.96 (d, $J=8.4$ Hz, 1H), 7.66 (ddd, $J=1.5$, 7.1, and 8.4 Hz, 1H), 7.52 (t, $J=7.5$ Hz, 1H), 7.28–7.19 (m, 2H), 4.81 (t, $J=6.9$ Hz, 2H), 3.06 (t, $J=6.9$ Hz, 2H), 2.72 (dd, $J=7.2$ and 14.4 Hz, 4H), 1.14 (t, $J=7.2$ Hz, 6H); ^{13}C NMR (75 MHz, $CDCl_3$) δ ppm 166.6, 163.2, 161.8, 154.6, 153.8, 144.2, 129.9, 129.8, 129.1, 128.0, 126.4, 124.7, 123.0, 123.0, 120.2, 116.5, 116.2, 114.6, 64.2, 51.0, 47.7, 29.7, 11.8. LRMS (ESI) m/z 380.3 $[M+H]^+$. HRMS (ESI) m/z calculated for $C_{22}H_{23}FN_3O_2^+$ $[M+H]^+$: 380.1769; found: 380.1814.

IL-33 protein expression and purification

IL-33₍₁₁₇₋₂₇₀₎ was cloned in an expression vector, pPROEX, as an N-terminal His-tag fusion protein in *E. coli* BL21(DE3). Cells were further grown for overnight at 20 °C after induction by 0.5 mM IPTG (isopropyl- β -D-thiogalactoside) when cell density (OD_{600}) reached 0.6. To obtain a uniform labeled ^{15}N IL-33₍₁₁₇₋₂₇₀₎, bacterial cells were grown in M9 minimal medium containing ^{15}N NH_4Cl . Cells were harvested and then re-suspended in lysis buffer (0.1 M Tris pH 7.4, 0.3 M NaCl, 1 mM β -mercaptoethanol, 0.1% TritonX100, and 0.1 mM phenylmethylsulfonyl fluoride). Cell lysis was performed by soni-

cation in an ice bath. Cell lysates were then centrifuged for 25 min at 10000 \times g and 4 °C. The pellet was discarded and the supernatant was then applied onto a 5 mL of pre-equilibrated HisPurTM cobalt resin column (Thermo Scientific Inc.) with 50 mM sodium phosphate pH 7.4, 300 mM NaCl, and 1 mM β -mercaptoethanol. After elution of cell lysates, the buffer was exchanged to 50 mM sodium phosphate pH 7.4, 300 mM NaCl, 1 mM β -mercaptoethanol, and 250 mM imidazole. The fusion protein was cleaved by thrombin protease at 4 °C in dialysis buffer (20 mM Tris pH 7.4, and 200 mM NaCl) for overnight. The IL-33 containing mixture was loaded into HisPurTM cobalt resin column, which was washed with 0.1 M Tris (pH 7.4), 0.3 M NaCl, and 1 mM β -mercaptoethanol. The bound protein was then eluted with 0.1 M Tris (pH 7.4), 0.3 M NaCl, 1 mM β -mercaptoethanol for 20 mL volumes. Proteins were loaded onto a Superdex S75 gel filtration column (16/60 GE Healthcare) in 20 mM sodium phosphate pH 6.8, 100 mM NaCl, 5 mM BME to yield pure IL-33 protein.

2D NMR spectroscopy

All measurements were acquired at 25 °C on Bruker 600 MHz NMR spectrometer equipped with a triple-resonance, pulsed field gradient probe (Bruker, Germany). A series of 2D 1H - ^{15}N HSQC spectra of IL-33₍₁₁₇₋₂₇₀₎ were measured in the absence and presence of each compound in same molar ratio. Data processing and analyzing were managed by using Topspin 3.1 program (Bruker, Germany) Chemical shift perturbations (CSPs) were calculated by using equation,

Where $\Delta\delta_{1H}$ and $\Delta\delta_{15N}$ denoted the proton and nitrogen chemical shifts differences.

Comparative molecular field analysis (CoMFA)

The CoMFA study was conducted for a new series of IL-33 inhibitors derived from BTB11086. The training set consisted of 13 new compounds and BTB11086. Chemical Shift Perturbation (CSP) of IL-33 signals is used as a surrogate for expressing the magnitude of the inhibition. To ensure the identical binding site in the same binding mode, we used CSP values of E121. To validate the resulting CoMFA model, 4 compounds were selected as a test set based on structural diversity by 2D similarity. All molecular modeling calculations were performed using SYBYL-X 2.1.1 (winnt_05x). Energy minimization for 3D conformation of each compound was performed using Tripos Force Field and Gasteiger-Huckel charge with Conjugate Gradient method with convergence criterion of 0.05 kcal/mol. The docked pose of BTB11086 from the previous docking study was used as a template to align the training and test compounds. The superimposition of molecules was processed by Distill Rigid. Two CoMFA descriptor fields, steric (Lennard-Jones) and electrostatic (Coulombic), were derived from the aligned dataset. Each potential field of CoMFA was calculated at each lattice intersection of a regularly spaced grid of 2.0 Å and the attenuation factor of 0.3. The regression analysis of the CoMFA field energies was performed using PLS (partial least squares) with LOO (leave-one-out) cross-validation, which was carried out to determine the optimum number of components. The modeling capability and prediction capability were evaluated by the non-cross-validated correlation coefficient (r^2) and the leave-one-out cross-validated correlation coefficient (q^2), respectively. In order to evaluate the predictive of the CoMFA model, the test set was used to predict CSP of non-model structures. The predictive r^2 (r^2_{pred}), obtained by using the formula, was used on models in the test set and was used to evaluate the predictive power of the CoMFA model.

Cell culture and reagents

Human mast cell-1 (HMC-1) was cultured with Iscove's modified Dulbecco's medium (IMDM, GE Healthcare HyClone™, USA) containing 10% fetal bovine serum (FBS) and 1% penicillin–streptomycin and incubated under 5% CO₂ at 37 °C. Cells were seeded at a concentration of 5 × 10⁵ cells/mL concentration in a 96-well plate with 100 nM of IL-33 and different concentrations (0.003–10 μM) of inhibitors for 24 hours.

Enzyme-linked immunosorbent assay (ELISA) for IL-6 production

The supernatant was harvested for analysis of IL-6 production by HMC-1. The amount of cytokine was determined using sandwich IL-6 enzyme-linked immunosorbent assay (ELISA) kit (BioLegend, Human IL-6 ELISA MAX™ Deluxe). Following the protocol provided from ELISA kit, each sample was analyzed with capture antibody and detection antibody. The monoclonal antibody pair was converted into a fluorescent signal by an avidin-horseradish peroxidase (HRP) that could be interpreted to the absorbance. The absorbance of plates was read on a microplate reader (SpectraMax® 190 Absorbance Plate Reader, Molecular Devices) at a wavelength of 450 nm. A standard curve was calculated from the concentration of 7 points increasing double time and used to determine the amount of IL-6 (pg/mL). For each condition, samples were analyzed in triplicates.

Statistical Analysis

Standard two-tailed t-test was used for statistical analyses. The calculated values for samples were expressed in mean ± STDEV (Standard deviation). p < 0.05 indicates statistical significance. GraphPad Prism software (Version 7.02) was utilized in every analysis

Acknowledgements

This work was supported by the National Research Foundation funded by the Ministry of Science, ICT & Future Planning (MSIP) and by the Ministry of Education of Korea (2014R1A4A1007304 and 2019R1A6A1A03031807)

Conflict of Interest

The authors declare no conflict of interest.

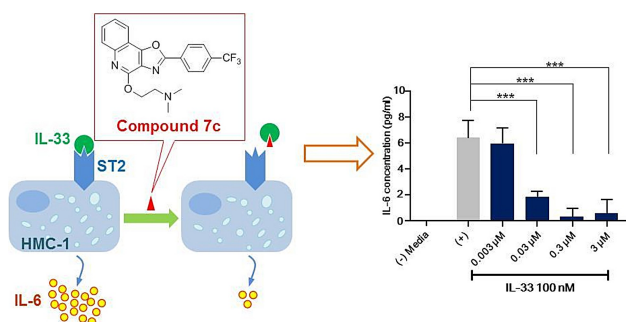
Keywords: Interleukin-33 · Allergy · Cytokine · Inhibitors · Oxazoloquinoline

- [1] a) J. Schmitz, A. Owyang, E. Oldham, Y. Song, E. Murphy, T. K. McClanahan, G. Zurawski, M. Moshrefi, J. Qin, X. Li, D. M. Gorman, J. F. Bazan, R. A. Kastelein, *Immunity* **2005**, *23*, 479–490; b) C. Moussion, N. Ortega, J. P. Girard, *Proc. Natl. Acad. Sci. USA* **2008**, *3*, e3331; c) M. Pichery, E. Mirey, P. Mercier, E. Lefrançois, A. Dujardin, N. Ortega, J. P. Girard, *J. Immunol.* **2012**, *188*, 3488–3495; d) H. Kouzaki, K. Iijima, T. Kobayashi, S. M. O'Grady, H. Kita, *J. Immunol.* **2011**, *186*, 4375–4387; e) R. Kakkar, H. Hei, S. Dobner, R. T. Lee, *J. Biol. Chem.* **2012**, *287*, 6941–

- 6948; f) Y. Haenuki, K. Matsushita, S. Futatsugi-Yumikura, K. J. Ishii, T. Kawagoe, Y. Imoto, S. Fujieda, M. Yasuda, Y. Hisa, S. Akira, K. Nakanishi, T. Yoshimoto, *J. Allergy Clin. Immunol.* **2012**, *130*, 184–194 e111; g) E. S. Cohen, I. C. Scott, J. B. Majithiya, L. Rapley, B. P. Kemp, E. England, D. G. Rees, C. L. Overed-Sayer, J. Woods, N. J. Bond, C. S. Veyssier, K. J. Embrey, D. A. Sims, M. R. Snaith, K. A. Vousden, M. D. Strain, D. T. Chan, S. Carmen, C. E. Huntington, L. Flavell, J. Xu, B. Popovic, C. E. Brightling, T. J. Vaughan, R. Butler, D. C. Lowe, D. R. Higazi, D. J. Corkill, R. D. May, M. A. Sleeman, T. Mustelin, *Nat. Commun.* **2015**, *6*, 8327.
- [2] a) S. Ali, M. Huber, C. Kollwe, S. C. Bischoff, W. Falk, M. U. Martin, *Proc. Natl. Acad. Sci. USA* **2007**, *104*, 18660–18665; b) A. A. Chackerian, E. R. Oldham, E. E. Murphy, J. Schmitz, S. Pflanz, R. A. Kastelein, *J. Immunol.* **2007**, *179*, 2551–2555.
- [3] a) S. Yasuoka, J. Kawanokuchi, B. Parajuli, S. Jin, Y. Doi, M. Noda, Y. Sonobe, H. Takeuchi, T. Mizuno, A. Suzumura, *Brain Res.* **2011**, *1385*, 8–17; b) F. Y. Liew, N. I. Pitman, I. B. McInnes, *Nat. Rev. Immunol.* **2010**, *10*, 103–110; c) A. M. Miller, *J. Inflamm. (Lond)* **2011**, *8*, 22.
- [4] G. Palmer, C. Gabay, *Nat. Rev. Rheumatol.* **2011**, *7*, 321–329.
- [5] a) G. Palmer, D. Talabot-Ayer, C. Lamacchia, D. Toy, C. A. Seemayer, S. Viatte, A. Finckh, D. E. Smith, C. Gabay, *Arthritis Rheum.* **2009**, *60*, 738–749; b) M. Li, Y. Li, X. Liu, X. Gao, Y. Wang, *J. Neuroimmunol.* **2012**, *247*, 25–31; c) H. R. Jiang, M. Milovanovic, D. Allan, W. Niedbala, A. G. Besnard, S. Y. Fukada, J. C. Alves-Filho, D. Togbe, C. S. Goodyear, C. Linington, D. Xu, M. L. Lukic, F. Y. Liew, *Eur. J. Immunol.* **2012**, *42*, 1804–1814; d) K. R. Bartemes, K. Iijima, T. Kobayashi, G. M. Kephart, A. N. McKenzie, H. Kita, *J. Immunol.* **2012**, *188*, 1503–1513; e) N. S. Grotenboer, M. E. Ketelaar, G. H. Koppelman, M. C. Nawijn, *J. Allergy Clin. Immunol.* **2013**, *131*, 856–865; f) J. L. Barlow, S. Peel, J. Fox, V. Panova, C. S. Hardman, A. Camelo, C. Bucks, X. Wu, C. M. Kane, D. R. Neill, R. J. Flynn, I. Sayers, I. P. Hall, A. N. McKenzie, *J. Allergy Clin. Immunol.* **2013**, *132*, 933–941; g) S. Kamijo, H. Takeda, T. Tokura, M. Suzuki, K. Inui, M. Hara, H. Matsuda, A. Matsuda, K. Oboki, T. Ohno, H. Saito, S. Nakae, K. Sudo, H. Suto, S. Ichikawa, H. Ogawa, K. Okumura, T. Takai, *J. Immunol.* **2013**, *190*, 4489–4499; h) T. Y. Halim, C. A. Steer, L. Matha, M. J. Gold, I. Martinez-Gonzalez, K. M. McNagny, A. N. McKenzie, F. Takei, *Immunity* **2014**, *40*, 425–435.
- [6] a) K. Oboki, T. Ohno, N. Kajiwara, H. Saito, S. Nakae, *Allergol. Int.* **2010**, *59*, 143–160; b) D. E. Smith, *Clin. Exp. Allergy* **2010**, *40*, 200–208; c) M. Milovanovic, V. Volarevic, G. Radosavljevic, I. Jovanovic, N. Pejnovic, N. Arsenijevic, M. L. Lukic, *Immunol. Res.* **2012**, *52*, 89–99.
- [7] Y. K. Kim, S. H. Cho, A. Ul Mushtaq, H. Cho, Y. W. Jung, Y. Byun, Y. H. Jeon, *Bull. Korean Chem. Soc.* **2016**, *37*, 117–118.
- [8] W. Blankenfeldt, I. D. Kerr, M. F. Giraud, H. J. McMiken, G. Leonard, C. Whitfield, P. Messner, M. Graninger, J. H. Naismith, *Structure* **2002**, *10*, 773–786.
- [9] K. J. Hodgetts, M. T. Kershaw, *Org. Lett.* **2003**, *5*, 2911–2914.
- [10] M. P. Doyle, B. Siegfried, J. F. Dellaria, *J. Org. Chem.* **1977**, *42*, 2426–2431.
- [11] a) M. R. Nimlos, D. F. Kelley, E. R. Bernstein, *J. Phys. Chem.* **1987**, *91*, 6610–6614; b) A. Held, D. F. Plusquellic, J. L. Tomer, D. W. Pratt, *J. Phys. Chem.* **1991**, *95*, 2877–2881; c) C. Charitos, C. Tzougraki, G. Kokotos, *J. Pept. Sci.* **2000**, *56*, 373–381; d) A. Gerega, L. Lapinski, M. J. Nowak, A. Furmanchuk, J. Leszczynski, *J. Phys. Chem. A* **2007**, *111*, 4934–4943; e) E. L. Lanni, M. A. Bosscher, B. D. Ooms, C. A. Shandro, B. A. Ellsworth, C. E. Anderson, *J. Org. Chem.* **2008**, *73*, 6425–6428; f) V. Arun, S. Mathew, P. P. Robinson, M. Jose, V. P. N. Nampoori, K. K. M. Yusuff, *Dyes Pigm.* **2010**, *87*, 149–157; g) G. Paramaguru, R. V. Solomon, S. Jagadeeswari, P. Venuvanalngam, R. Renganathan, *Eur. J. Org. Chem.* **2014**, 753–766; h) C. Mugnaini, A. Brizzi, A. Ligresti, M. Allara, S. Lamponi, F. Vacondio, C. Silva, M. Mor, V. Di Marzo, F. Corelli, *J. Med. Chem.* **2016**, *59*, 1052–1067.
- [12] A. Lingel, T. M. Weiss, M. Niebuhr, B. Pan, B. A. Appleton, C. Wiesmann, J. F. Bazan, W. J. Fairbrother, *Structure* **2009**, *17*, 1398–1410.
- [13] J. Senger, J. Melesina, M. Marek, C. Romier, I. Oehme, O. Witt, W. Sippl, M. Jung, *J. Med. Chem.* **2016**, *59*, 1545–1555.
- [14] G. Khose, S. Shinde, A. Panmand, R. Kulkarni, Y. Munot, A. Bandyopadhyay, D. Barawkar, S. N. Patil, *Tetrahedron Lett.* **2014**, *55*, 2671–2674.

Manuscript received: August 4, 2021
Revised manuscript received: September 14, 2021
Accepted manuscript online: September 22, 2021
Version of record online: ■■■, ■■■■

FULL PAPER



The oxazolo[4,5-c]-quinolinone analog **7c** is the first small-molecule inhibitor of interleukin-33, demonstrated by its binding to the interface of IL-33 and

ST2 in a 2D NMR study and a strong inhibition of interleukin-6 production in human mast cells.

Y. Kim, C. Ma, S. Park, Y. Shin -, T. Lee, J. Paek, K. Hoon Kim, G. Jang, H. Cho, S. Son, S.-H. Son, Prof. K. Yong Lee, Prof. K. Lee, Prof. Y. Woo Jung*, Prof. Y. Ho Jeon*, Prof. Y. Byun*

1 – 12

Rational Design, Synthesis and Evaluation of Oxazolo[4,5-c]-quinolinone Analogs as Novel Interleukin-33 Inhibitors